WELDING RESEARCH

SUPPLEMENT TO THE WELDING JOURNAL, APRIL, 1985

Sponsored by the American Welding Society and the Welding Research Council
TECHNICAL PAPERS EDITOR: T.P. SCHOONMAKER

The Relationship Between Grain Size and Microfissuring in Alloy 718

Microfissuring is linearly dependent on grain size

BY R. G. THOMPSON, J. J. CASSIMUS, D. E. MAYO AND J. R. DOBBS

ABSTRACT. The weldability of certain high temperature alloys is limited by microfissuring in the weld heat-affected zone. Experience indicates that the microfissuring problem is significantly increased in metals and large grain size.

The study described in this paper examined the microfissuring susceptibility of wrought alloy 718 as a function of grain size. The spot varestraint test was used to microfissure a grain size range of 20 μ (ASTM #8) to 200 μ (ASTM #1) at three different strain levels.

It was found that microfissuring susceptibility was linearly dependent on grain size. Microfissuring increased with increasing grain size at the same rate for three different strain levels.

Introduction

The weldability of high temperature alloys is often limited either by strain age cracking or heat-affected zone (HAZ) microfissuring. The microfissuring problem in alloys such as 718 (composition in Table 1) is accentuated by alloy additions which reduce the strain age cracking problem. An element such as niobium (columbium is synonymous with Nb), when added to certain γ' strengthened nickel alloys, produces γ'' strengthening which is resistant to strain age cracking.

R. G. THOMPSON, J. J. CASSIMUS, D. E. MAYO, and J. R. DOBBS are associated with the School of Engineering at The University of Alabama in Birmingham.

Table 1—Alloy 718 Composition, %

C	0.04	Ni	52.42
Mn	0.10	Cr	18.35
Fe	18.95	Al	0.60
S	0.003	Ti	1.00
Si	0.16	Co	0.10
Cu	0.08	Mo	2.98
Nb + TA	5.22		

However, the Nb addition also results in the precipitation of niobium carbides. These carbides act as concentrated sources of Nb during rapid heating; the result is the formation of intergranular eutectic-type liquid. This intergranular liquid is a prerequisite for HAZ microfissuring (Ref. 1). Figure 1 illustrates the microfissure sequence described by Thompson and Genculu (Ref. 1).

Many studies have looked at the possible effects of impurity and alloy elements and precipitates on microfissuring (Ref. 1). Of these, only one referred to the effect of grain size. This was that of Morrison *et al.* (Ref. 2) who reported that metal with a grain size greater than ASTM #2 showed a greater tendency to micro-

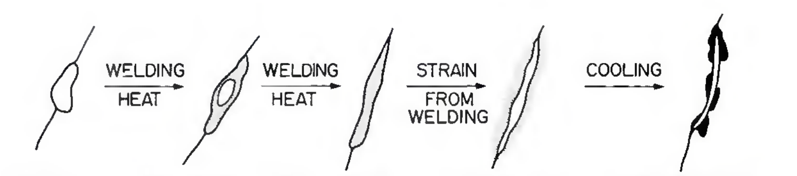

Fig. 1—Microstructure—microfissure sequence

Table 2—Grain Growth in Wrought Alloy 718

Time, minutes	Temperature, °F 1800	1900	1950	2000	2100	2150
Initial	15[a]	15	15	15	15	15
5	—	—	35	—	50	60
15	20	40	55	80	90	—
30	25	50	—	90	110	110
60	40	70	80	130	150	—
90	50	90	—	150	—	—
180	—	—	—	—	180	180
1440	—	—	130	—	—	200
5760	—	—	150	—	—	—
7200	—	—	—	—	—	200

(a) Average grain size in microns (10^{-6} m).

Table 3—Grain Growth Schedule

10 μ grain size	As received[a]
32 μ grain size	30 s at 2130°F in flowing argon; quenched in flowing argon
60 μ grain size	5 min at 2130°F in flowing argon; quenched in flowing argon
200 μ grain size	24 h at 2130°F in vacuum; quenched in water

(a) As-received structure had fine dispersion of $Ni_3Nb(\delta)$ used to pin a thermally unstable, recrystallized grain structure.

fissure than smaller grain sizes. However, they found no correlation between grain size variance and microfissuring for grain sizes less than ASTM #2.

Welding experience with alloy 718 has shown that material with large grain size (such as encountered in castings) is more prone to microfissure than material (such as used for wrought parts) with smaller grains. Such observations raise many questions about the relationship between grain size and microfissuring. Is there a true grain size effect or is the observed microfissuring susceptibility related to some other aspect of the processing technique? For example, might cast material (compared to the wrought material) be more microfissure-prone due to the greater segregation attendant with that process? The microfissuring may be mistakenly associated with grain size, because it is a more prominent characteristic of the process than is segregation.

Even in specimens taken from the same heat of material, it might be difficult to isolate a true grain size effect from other, simultaneous, changes in the material. It would be tempting to take a single heat of material and produce a grain size variation by heat treating over a temperature range. Low annealing temperatures could be used to produce small grains and higher temperatures for larger grains. This is practical since grain size is strongly dependent on temperature. However, intergranular segregation (Ref. 3) and carbide morphology (Ref. 4) are also dependent on temperature in the range which would be used for grain growth. Valdez and Steinman (Ref. 5) have also shown that microfissuring susceptibility in alloy 718 increases with increasing annealing temperature between 1750 and 1950°F (954 and 1066°C).

It is evident that in order to establish the relationship between microfissuring and grain size, the experimental approach must be carefully planned. The results must also be interpreted with attention to metallurgical changes which

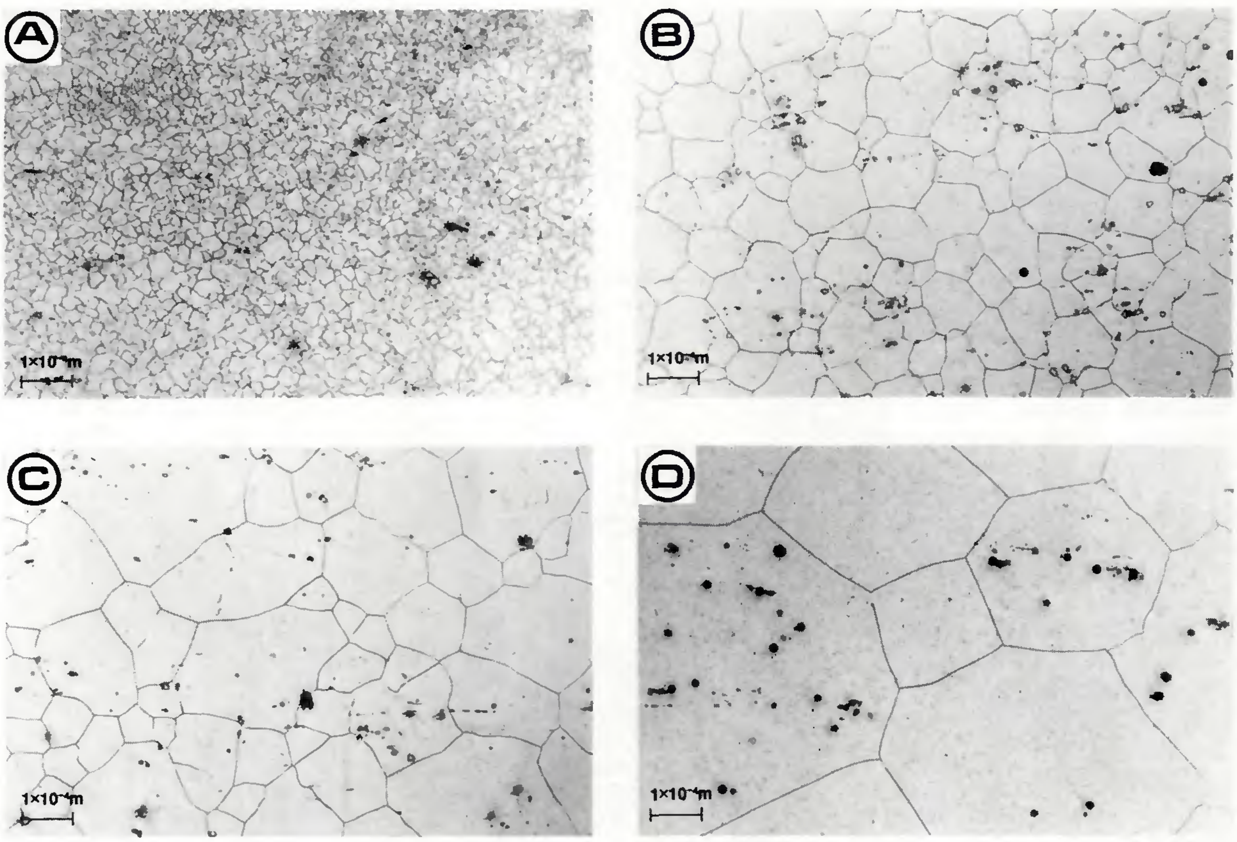

Fig. 2—Base metal grain size range: A—as received; B—30 s at 2130°F (1166°C); C—5 min at 2130°F; D—24 h at 2130°F

might be superimposed on the variation in grain size.

This paper reports the results of a study whose experimental plan was sensitive to the above pitfalls and possible shortcomings. A single heat of alloy 718 was used for all testing. Wrought material was used to minimize segregation, and grain growth was accomplished at a single temperature using different annealing times. Finally, all specimens were quenched from the annealing temperature to prevent complication from the precipitation of secondary phases other than carbides. Results are presented which quantitatively establish a relationship between microfissuring and grain size in wrought alloy 718.

Experimental Procedure and Results

Grain Growth Methodology

The method used to produce an acceptable grain size range, while at the same time minimizing secondary metallurgical effects, was a critical step in this investigation. The starting material was a single ⅛ in. (3.2 mm) thick sheet of alloy 718 whose composition is given in Table 1. It was mill processed to an average grain size of 10 μ (ASTM #9). The grain growth rates over a range of annealing temperatures were determined, and the data are presented in Table 2.

A grain growth annealing temperature of 2130 ± 10°F (1166 ± 6°C) was chosen for the following reasons:

1. The high temperature would maximize grain growth.
2. Although the temperature was high, it was well below the carbide-liquation temperature of approximately 2150°F (1176° C).
3. This annealing temperature was well above the solutioning temperature for precipitates such as γ', γ'', and $Ni_3Nb(\delta)$. (The solutioning behavior for Laves phase* was not known, although it was known that Nb and Ti carbides would resist solutioning.)
4. The high temperature would minimize intergranular segregation.
5. The high temperature would maximize homogenization.

The grain growth schedule is given in Table 3, and the results are shown in Fig. 2. The short time grain growth cycles of 30 seconds(s) and 5 minutes (min) were made with an induction furnace to minimize heat-up and cool-down time. Flowing argon was used both as a protective environment and as a quenchant. The longer grain growth cycles were made by sealing the specimens in evacuated quartz tubing and heating in a box furnace. These specimens were quenched in water to prevent precipitation of unwanted phases during cooling.

Spot Varestraint Machine

A spot varestraint machine (Tigamajig), designed after the one reported by Savage, Nippes, and Goodwin (Ref. 6) was used in the present study to produce HAZ microfissures. Since HAZ microfissures are thought to occur due to thermal stress during cooling, the spot varestraint test was programmed to stimulate this behavior.

The experimental setup is shown in Fig. 3. In order to simulate the thermal-stress cycle of microfissuring, the dynamics of the welding power source and the pneumatic piston were carefully orchestrated. Figure 4 shows the effects of possible combinations of welding machine-pneumatic piston dynamics on microfissuring.

If the action of the pneumatic piston lags the cut-off of the welding machine, fissures appear only in the solidifying weld pool — Fig. 4A. When the welding machine cut-off is delayed, stress is applied by the piston as the HAZ cools such that microfissures form in the HAZ and propagate slightly into the solidifying weld pool — Fig. 4B. However, if the cut-off of the welding machine is delayed too long, microfissures form only in the HAZ, because they are unable to propagate into the fully molten weld pool which has not yet begun to cool — Fig. 4C.

The dynamic relationship between welding machine and piston was controlled by the amount of resistance in a resistance-capacitance (RC) discharge circuit. The time lag of this circuit determined the welding machine cut-off relative to the actuation of the pneumatic piston of the spot varestraint machine. This set-up allowed the microfissuring pattern of Fig. 4B to be reproducibly made and, thus, simulate a typical HAZ microfissuring event.

The geometry of the spot varestraint specimens is given in Fig. 5. Test material was conserved by welding extension tabs onto the central test specimen as shown in Fig. 5. A welding jig was designed for attaching the extension tabs. This jig had copper hold-down strips to minimize the HAZ of the fabrication welds. It also prevented the heat generated by this welding operation from changing the

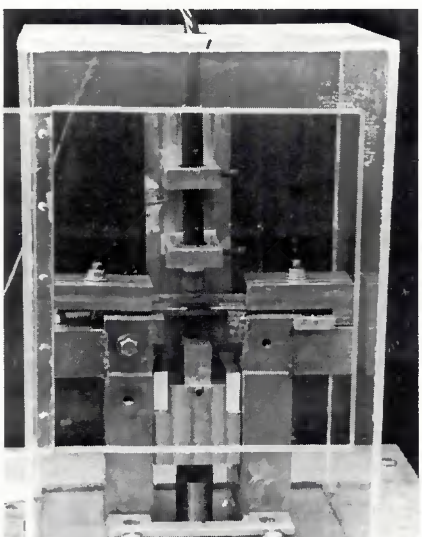

Fig. 3 — Spot varestraint test stand

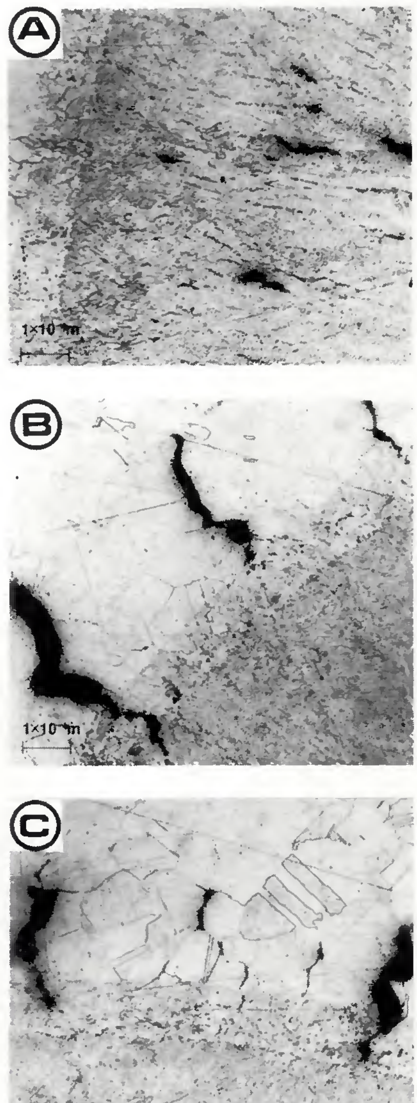

Fig. 4 — Effect of test stand coordination on microfissure location: A — application of strain too slow; B — application of strain at correct time; C — application of strain too fast

*Laves phase — a "size factor compound" where one atom is 20 to 30% smaller than the other, enabling them to pack together in crystal structures more efficiently than if they were the same size.

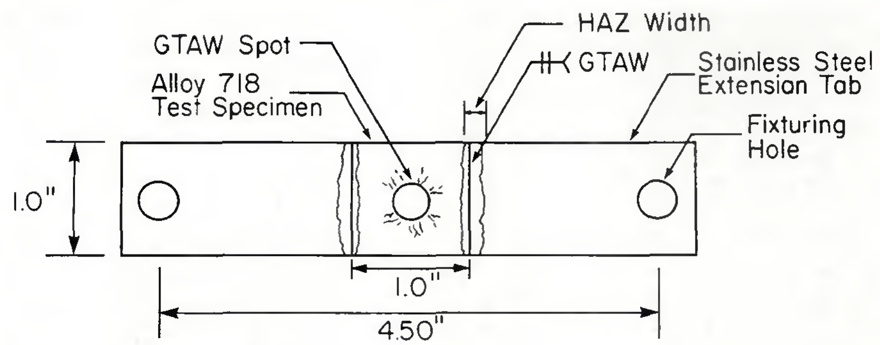

Fig. 5 — Spot varestraint test specimen

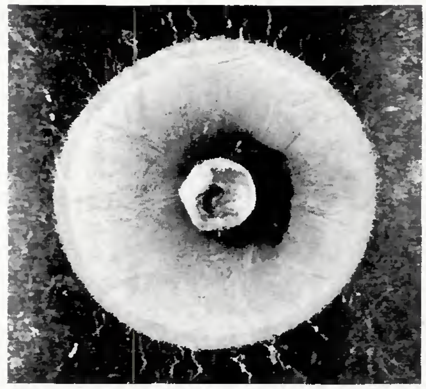

Fig. 7 — An example of the microfissure pattern produced in the spot varestraint test. Specimen 23 (3% strain, 170 μ grain size)

carefully prepared properties of the specimens.

The spot varestraint test parameters are given in Table 4. Three strain levels were used by varying both the bending radius and the length of travel of the piston. The tangential strains ($\epsilon = \frac{t}{2r}$) as determined from the radius of the bending die, were 1, 3, and 5%. (Figure 6 illustrates the relative magnitudes of strain applied in these tests.)

Following the spot varestraint test, the specimens were polished and electrolytically etched in oxalic acid. A typical microfissure pattern, as revealed by this process, is shown in Fig. 7. The total length of microfissures was measured using a micrometer eyepiece with a moveable crosshair at ×100 magnification. The results of this analysis are given in Table 5.

Discussion

Grain Size

The base metal grain size, as shown in Fig. 2, should not be correlated directly with spot varestraint microfissuring data. Heat-affected zone grain growth occurs during the weld cycle and thus alters the grain size prior to microfissuring. Figure 8 shows the HAZ grain size gradient for the most exaggerated case in our experiments. Since microfissures are initiated and grow in the HAZ, it is important that the HAZ grain size be correlated with microfissuring. A problem with determining a HAZ grain size is that a grain size gradient exists. It was decided to average the grain sizes in the HAZ over which the microfissures extend. This average HAZ grain size, which was susceptible to microfissuring, is given in Table 5.

The correlation between microfissuring and HAZ grain size is shown in Fig. 9. Although the data are not sufficient in numbers for a statistical analysis, the straight lines drawn through the data seem to represent the general trend adequately. Notice that the curves maintain approximately the same slope for all strain levels. This indicates that the relationship between grain size and microfissuring is independent of the amount of strain applied to the HAZ. The slope of

Table 5—Varestraint Test Results

Specimen Number	Base metal grain size, μ	HAZ grain size, μ	Augmented strain, %	Total crack length, 10^{-6}, m
20	14	20	1	8005
27	9	20	1	9410
26	9	21	3	16963
19	5	16	5	18834
28	9	20	5	23269
2	30	37	1	10559
31	32	37	1	13454
3	33	37	3	23152
4	34	40	5	29204
8	45	55	1	16047
7	69	80	3	22137
9	71	74	5	31915
22	180	208	1	26415
29	197	250	1	22776
23	158	222	3	35730
25	220	193	3	36096
24	235	177	5	41344
30	196	194	5	47716

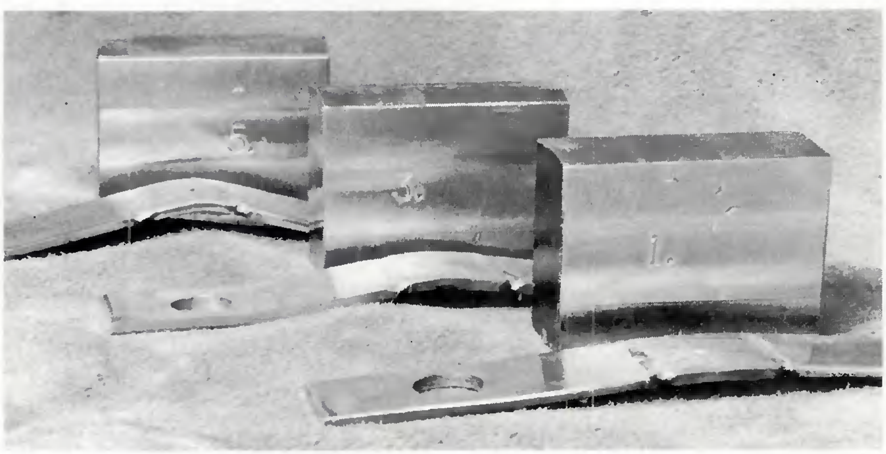

Fig. 6 — Specimens showing typical plastic strain and the associated bending dies. Augmented strains from front to back are 1%, 3%, and 5%

Table 4—Varestraint Test Parameters

Welding current, A	65
Welding voltage, V	12.5
Arc on time, s	10
Argon shielding, cfh	30
Electrode[a] to work distance, mm (in.)	6.2 (0.245)

(a) 2% thoria W electrode, 1/16 in. (1.59 mm) diameter, 60 deg included angle

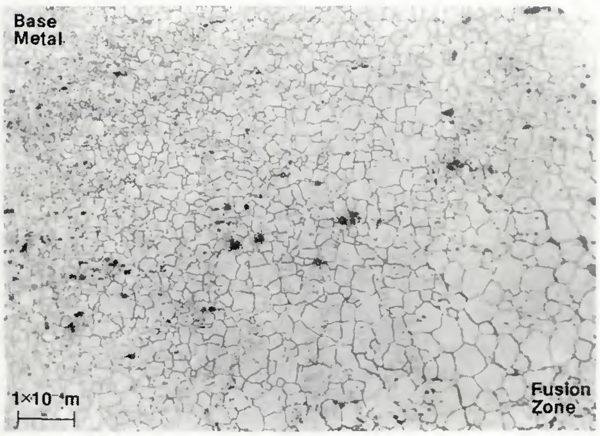

Fig. 8 — Gradient in HAZ grain size for most temperature sensitive condition

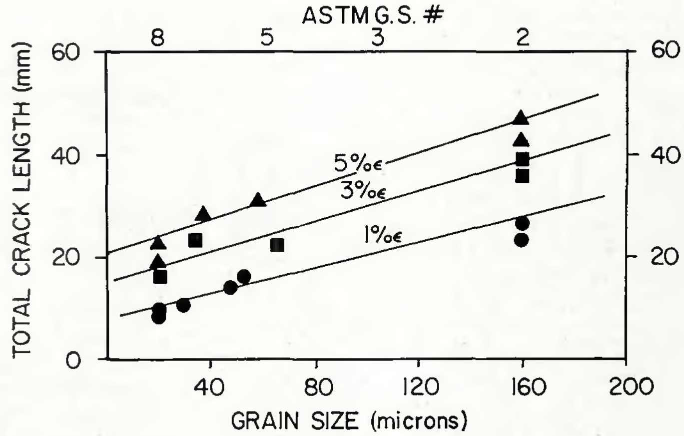

Fig. 9 — Relationship between HAZ grain size and microfissuring (based on total microfissure length per specimen)

the curve also reveals that alloy 718 experienced a 0.4% increase in microfissuring per micron increase in grain size.

Microfissure Distribution

The specimen is stressed in a combination of bending and uniaxial tension due to the method of gripping the specimen in the test stand. The uniaxial tension portion of the stress has the usual tensile and shear components of the stress state. In order to determine the distribution of cracks relative to the tensile and shear components of stress, the specimen was divided into 90 deg quadrants as shown in Fig. 10. Each quadrant contains the same stress distribution, and hence the data from each quadrant can be summed and presented in a 0–90 deg format.

Figure 11 presents the total crack length as a function of stress distribution for the 32 μ grain size specimen. The other grain sizes reacted in a similar manner to that shown in Fig. 11.

The peak in microfissuring on the maximum shear axis is prominent for all grain sizes at all strain levels. The data strongly suggest that a microfissuring mechanism is related to the shear component of the stress state.

Microfissuring Mechanism

Our research has identified three items which should be considered when developing a microfissuring model for alloy 718:

1. Intergranular liquid is a prerequisite for microfissuring (Ref. 2).
2. The magnitude of microfissuring is dependent on grain size.
3. Microfissuring is sensitive to the shear component of the stress state.

Item one calls to attention the need to consider the intergranular liquid distribution in a microfissuring mechanism. Borland (Ref. 7) used Smith's (Ref. 8) intergranular liquid distributions to develop a theory of super-solidus cracking in welds. The idea that grain boundary liquid produces crack susceptibility by reducing metal-to-metal contact area is widely accepted. Observations and results from the present study also support this idea. However, the liquid phase distribution theory does not explain the observation of a crack distribution dependence on shear stress. Nor does it sufficiently explain a microfissuring dependence on grain size.

A study by Williams and Singer (Ref. 9) considered the effect of grain boundary sliding on cracking in the presence of an intergranular liquid. They hypothesized that grain boundary sliding produced stress concentrations that aided crack propagation. They also theorized that grain boundary sliding and the associated stress concentration were maximum on the maximum shear axis. This is interesting in light of the present finding that microfissuring also experiences a maximum on the maximum shear axis.

Grain boundary sliding is usually associated with elevated temperature and slow strain rates. However, Williams and Singer (Ref. 9) reviewed several studies, which showed that grain boundary sliding is a primary deformation mode when intergranular liquid is present. Work has also been presented that shows grain boundary sliding would be an effective mechanism for initiation of microfissures

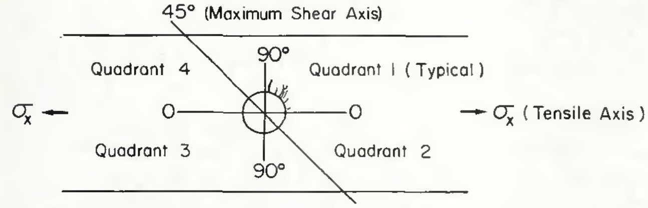

Fig. 10 — Specimen orientation relative to the applied stress during the spot varestraint test

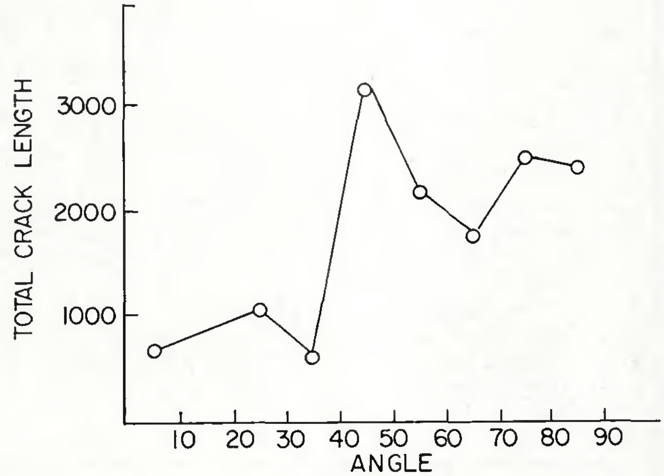

Fig. 11 (right) — Distribution of microfissuring relative to the orientation of applied stresses at grain boundary triple points (Ref. 10). Once these microfissures initiate, they could easily propagate through the intergranular liquid.

The effect of grain size on microfissuring could be related to both the liquid distribution and grain boundary sliding. A large grain size would lead to a thicker liquid layer than a small grain size if the same volume of liquid is present in both cases. A large volume fraction of intergranular liquid could increase the temperature range and time duration during which liquid wets the grain boundary faces under nonequilibrium freezing conditions. This would lead to increased microfissuring susceptibility. A large grain size would also cause a longer interface sliding length, which would lead to larger stress concentrations, larger strains at grain boundary triple points, and increased crack initiation due to grain boundary sliding. Thus, a large grain size would be detrimental to both aspects of microfissuring.

Summary

Based on the foregoing results, it is postulated that grain boundary sliding opens a triple point crack which propagates a microfissure through the liquid distributed on the crack face. An intergranular liquid distribution, which covers the grain boundary faces, is required for both significant grain boundary sliding and microfissure propagation from the grain boundary triple point. Both the detrimental liquid distribution on the grain boundary faces and the stress concentrations due to grain boundary sliding are accentuated by a large grain size.

The key to the microfissure process is the intergranular liquid distribution. Microfissuring could probably be eliminated, if the liquid phase were prevented from wetting the grain boundary faces. The control of this liquid wetting could be accomplished through the intentional segregation of some beneficial element to the grain boundaries prior to welding. It could also be controlled by preweld processing which prevents NbC precipitation at grain boundaries.

Conclusion

Increasing grain size gradually increases microfissuring susceptibility at the rate of 0.4% per micron increase in grain size. The increases in microfissuring susceptibility with increasing ASTM grain size number are as follows:

ASTM no.	Microfissure increase, %
9	Baseline
7	5%
5	12%
3	38%
1	82%
00	175%

The relatively large increase in microfissuring between ASTM numbers 3 and 1 roughly corresponds to industry experience with microfissuring in this grain size range.

Increased microfissuring susceptibility due to grain growth in the heat-affected zone will only be a problem in base metal with a small grain size (less than 50 microns (ASTM no. 5)). Larger base metal grain sizes show little or no tendency toward HAZ grain growth.

The shear component of stress appears to accentuate microfissuring. This observation may be attributed to a grain boundary sliding mechanism of microfissure initiation. The reason that large grain size accentuates microfissuring could partially be explained by its promotion of grain boundary sliding stress.

Acknowledgments

The authors gratefully acknowledge the National Aeronautics and Space Administration for its support of this research through grant NAS8-34962. Special recognition goes to Bob Rowe of the Marshall Space Flight Center for his many helpful suggestions and comments. The authors also thank Ed Cables and Dennis Phillips for dedicated work in preparation of this research.

References

1. Thompson, R. G., and Genculu, S., 1983. Microstructural evolution in the HAZ of Inconel 718 and correlation with the hot ductility test. *Welding Journal* 62 (12): 337-s to 345-s.

2. Morrison, T. J., Shira, C. S., and Weisenberg, L.A. 1969. The influence of minor elements on alloy 718 weld microfissuring. *Effects of minor elements on the weldability of high-nickel alloys,* p. 47. New York: Welding Research Council.

3. White, C. L., Schneibel, J. H., and Padgett, R. A. 1983. High temperature embrittlement of Ni and Ni-Cr alloys by trace elements. *Met. Trans.* 14A: 595.

4. Airey, G. P. 1980. Microstructural aspects of the thermal treatment of Inconel alloy 600. *Metallography* 13: 21.

5. Valdez, P. J., and Steinman, J. B. 1969. Effect of composition and thermal treatment on the weldability of nickel-base Alloy 718. *Effects of minor elements on the weldability of high-nickel alloys,* p. 93. New York: Welding Research Council.

6. Savage, W. F., Nippes, E. F., and Goodwin, G. W. 1977. Effect of minor elements on hot-cracking tendencies of Inconel 600. *Welding Journal* 56(8): 245-s to 253-s.

7. Borland, J. C. 1960. Generalized theory of super-solidus cracking in welds (and castings). *British Welding Journal* 7: 526.

8. Smith, C. S. 1948. Grains, phases, and interfaces: an interpretation of microstructure. *Trans. A.I.M.M.E.,* p. 175.

9. Williams, J. A., and Singer, A. R. E. 1968. Deformation, strength and fracture above the solidus of temperature. *Journal of the Inst. of Metals* 96: 5.

10. William, J. A. and Singer, A. R. E. 1966. A review of the mechanisms of hot short cracking. *The Journal of the Australian Institute of Metals* 11(1): 2.